Nanoscale Res Lett (2009) 4:680–683
DOI 10.1007/s11671-009-9297-7

NANO EXPRESS

Fabrication of Antireflective Sub-Wavelength Structures on Silicon Nitride Using Nano Cluster Mask for Solar Cell Application

Kartika Chandra Sahoo · Men-Ku Lin · Edward-Yi Chang · Yi-Yao Lu · Chun-Chi Chen · Jin-Hua Huang · Chun-Wei Chang

Received: 7 February 2009 / Accepted: 5 March 2009 / Published online: 22 April 2009
© to the authors 2009

Abstract We have developed a simple and scalable approach for fabricating sub-wavelength structures (SWS) on silicon nitride by means of self-assembled nickel nanoparticle masks and inductively coupled plasma (ICP) ion etching. Silicon nitride SWS surfaces with diameter of 160–200 nm and a height of 140–150 nm were obtained. A low reflectivity below 1% was observed over wavelength from 590 to 680 nm. Using the measured reflectivity data in PC1D, the solar cell characteristics has been compared for single layer anti-reflection (SLAR) coatings and SWS and a 0.8% improvement in efficiency has been seen.

Keywords Sub-wavelength Structure · Solar cell · SWS fabrication · Reflectance · Anti-reflective coatings

Introduction

The antireflection coating has become a key feature for solar cell design [1–4]. Many researchers have investigated double-layer antireflection (DLAR) coatings because single-layer antireflection coatings (SLAR) are not able to cover a broad range of the solar spectrum [5, 6]. Unfortunately, multilayer ARCs are expensive to fabricate owing to the stringent requirement of high vacuum, material selection, and layer thickness control. Additionally, thermal mismatch induced lamination and material diffusion of the multilayer ARCs limit the device performance at high power densities.

An alternative to multilayer ARCs are the sub-wavelength structured (SWS) surface with dimensions smaller than the wavelength of light [7]. In publications concerning broadband or solar anti-reflective surfaces, [8–11] the principle to achieve the necessary low refractive indices is always the same: substrate material is mixed with air on a sub-wavelength scale. To date, a wide variety of techniques have been investigated for texturing multi-crystalline (mc) silicon cells [12]. One of the promising options is surface texturing by dry etching technique. Some groups have succeeded in fabricating uniform textures with a submicron scale on mc-Si wafers by reactive ion etching and applied to the Si solar cells [13, 14]. Unfortunately, there is not much report on texturization of silicon nitride and the optical properties of submicron textures on silicon nitride for the application of solar cells.

In this study, we fabricated sub-wavelength structure on antireflection coating layers instead of semiconductor layer on solar cell. The main motivation behind this lies in the fact that the sub-wavelength structures will act as a second ARC layer with an effective refractive index so that the total structure can perform as a DLAR layer. Thus we can cost down the deposition of 2nd ARCs layer can be saved with better or comparable performance as that of a DLAR solar cell. We fabricate the silicon nitride sub-wavelength structures using the mask less RIE technique on silicon substrate and explore the reflection properties of the texturing structures through spectroscopic measurements [15].

K. C. Sahoo · E.-Y. Chang (✉) · Y.-Y. Lu · C.-C. Chen
Department of Materials Science and Engineering,
National Chiao Tung University, Hsinchu, Taiwan
e-mail: edc@mail.nctu.edu.tw

M.-K. Lin · J.-H. Huang
Department of Materials Science and Engineering,
National Tsing Hua University, Hsinchu, Taiwan

C.-W. Chang
Taiwan Semiconductor Manufacturing Company Ltd,
Hsinchu, Taiwan

Experiment

The fabrication procedure is schematically shown in Fig. 1. First of all the polished (100) silicon was cleaned with dilute HF to remove the native oxide. A layer of (200 ± 0.05) nm thick silicon nitride (Si_3N_4) was then deposited on a polished (100) silicon wafer by plasma enhanced chemical vapor deposition (PECVD) technique. A nickel film with a thickness of (15 ± 0.05) nm was then evaporated on the silicon nitride surface using an E-beam evaporating system. The nickel film was then rapid thermal annealed (RTA) under the forming gas (mixture of H_2 and N_2) with a flow rate of 3 sccm at 850 °C for 60 s to form nickel clusters, which served as the etch masks for silicon nitride. The sample is then etched by ICP etching with bias power of 200 watt to form the sub-wavelength structures using a gas mixture of CF_4/O_2 with flow rate of 60 and 6 sccm for CF_4 and O_2, respectively. To remove the residual nickel mask, the sample was dipped into pure nitric acid (HNO_3) solution for 5 min at room temperature. The diameter and density of the fabricated sub-wavelength structures were nearly the same as those of the nickel cluster masks, while the height was controlled by the etching time. The morphology of SWS was analyzed by scanning electron micrograph (SEM). The reflectance of the SWS were measured using an n&k analyzer (model: 1280, N&K Tech. Inc.).

Results and Discussion

Figure 2a shows the SEM images of the nickel nanoclusters formed after rapid thermal annealing at 850 °C for 60 s. The diameters of the nanoclusters were varied from 160 to 200 nm. Figure 2b shows the SEM image of the fabricated SWS on silicon nitride after ICP dry etching for 120 s. From Fig. 2b, the height of the silicon nitride SWS was measured to be 140–150 nm, diameters of fabricated SWSs were varied from 160–200 nm, which were same as that of nickel nanoclusters.

Figure 3 shows the comparison of the measured reflectivity from a polished silicon wafer with 69.1 nm silicon nitride SLAR coating and fabricated silicon nitride SWS on silicon wafer. The flat silicon substrate exhibits high-reflection >35% for visible and near infrared wavelengths, silicon nitride SLAR coatings exhibits low-reflection <20% for long wavelengths 700 nm and high-reflection >35% for shorter wavelengths 400 nm, and silicon nitride/MgF_2 DLAR coatings exhibits low-reflection <10% for long wavelengths 700 nm and high-reflection >20% for short wavelength 400 nm, while the SWS gratings show reduced reflection of <10% for long wavelengths 700 nm and shorter wavelengths 400 nm. The reflection is further reduced to <1% for wavelengths around 580–680 nm. The silicon nitride SWS gratings exhibit lower reflection than colloid-based antireflection coatings on crystalline silicon solar cells, [16] other SWS ARCs made by lithographic techniques with typical reflection of ~2–10% [8, 17–20], Additionally, optimization of the height and non-etched part of silicon nitride of SWS will facilitate further improvement of the antireflection performance.

AR design has been characterized by its average residual reflectance R_{av}, [21] which is defined by the equation

$$R_{av} = \frac{1}{\lambda_u - \lambda_l} \int_{\lambda_l}^{\lambda_u} R(\lambda) d\lambda, \quad (1)$$

where $R(\lambda)$ is the reflectance of the design and λ_l and λ_u are the lower and upper wavelength of the design window. The average residual reflectance R_{av} has been calculated using the Eq. 1 by taking the wavelength range from 350 to 1000 nm into consideration for a bare Si, SLAR w/Si_3N_4

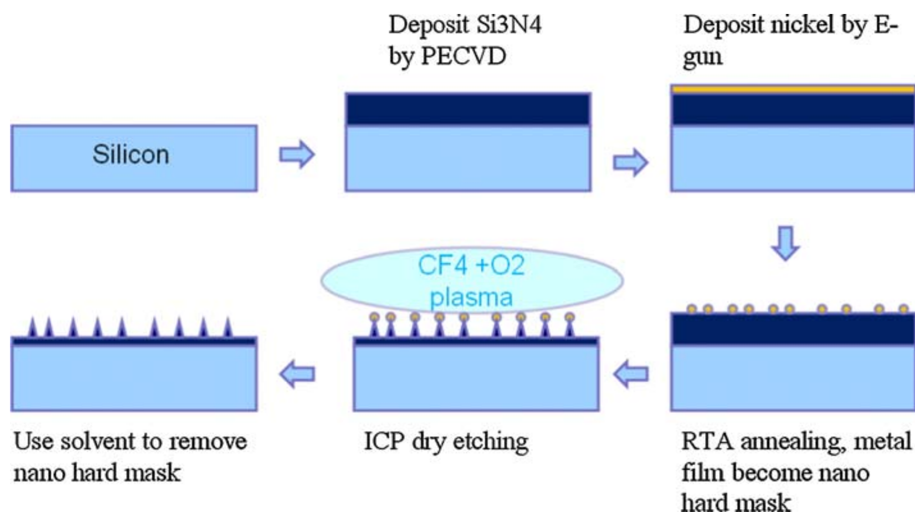

Fig. 1 Schematic illustration of the process steps for fabricating SWS gratings on silicon nitride

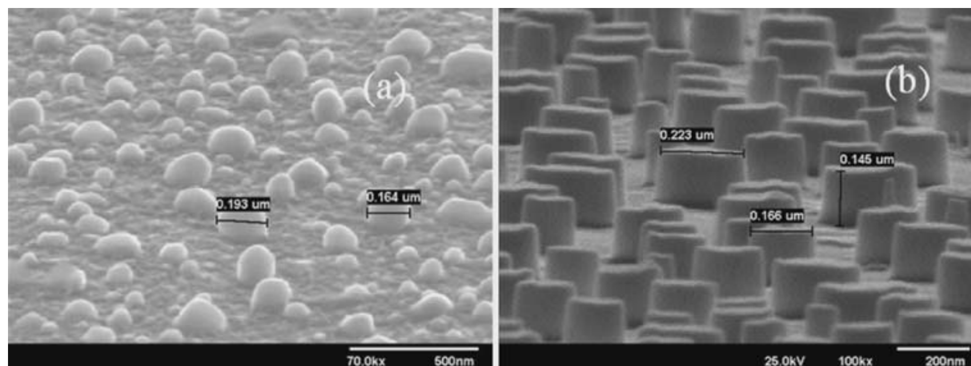

Fig. 2 SEM Images **a** Nickel nano-clusters formed after rapid thermal annealing at 850 °C for 60 s, **b** Fabricated silicon nitride SWSs after dry etching with ICP for 120 s

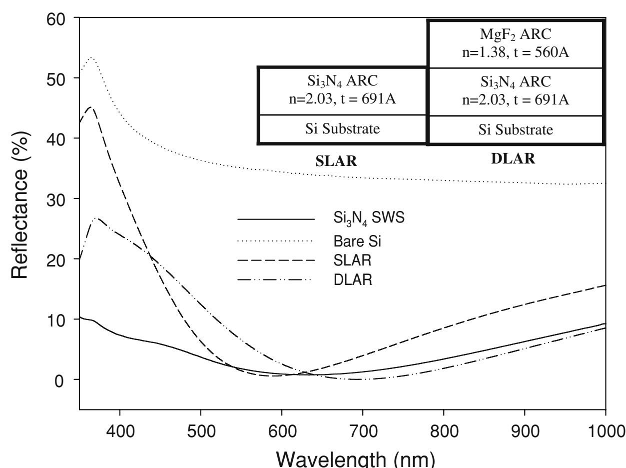

Fig. 3 Measured optical reflectivity at normal incidence for bare (100) silicon wafer, fabricated 140 ~ 150 nm height silicon SWS, SLAR w/silicon nitride of 69.1 nm deposited on silicon wafer and DLAR w/69.1 nm silicon nitride and 56 nm MgF_2 deposited on silicon wafer

Table 1 Average residual reflectivity calculated by the Eq. 1 for measured reflectance of bare silicon, 69.1 nm silicon nitride deposited on silicon, 69.1 nm silicon nitride and 56 nm MgF_2 double layer deposited on silicon and 140–150 nm silicon nitride SWS fabricated on silicon

Structure	Average residual reflectivity, R_{av} (%)
Silicon	35.61
Silicon nitride SLARC	11.22
Silicon nitride/MgF_2 DLARC	7.64
Silicon nitride SWS	4.28

SLARC Single layer anti-reflective coating, *DLARC* Double layer anti-reflective coating, *SWS* Sub-wavelength structure

thickness of 69.1 nm, DLAR of Si_3N_4/MgF_2 w/thickness of 69.1 nm and 56 nm, respectively for Si_3N_4 and MgF_2, and fabricated Si_3N_4 SWS. The results are shown in Table 1. From Table 1 it is clear that the silicon nitride SWS has the lowest average residual reflectance of 4.28% as compared to bare silicon, 69.1 nm silicon nitride SLAR coatings and DLAR coating with 69.1 nm silicon nitride and 56 nm MgF_2. For the consideration of working wavelength region of silicon-based solar cells, the pyramid structure with height of 140–150 nm is suitable as the antireflective structure and believed to increase the solar cell performance as compared to solar cell w/SLAR structure.

To investigate the performance of silicon nitride SWS before fabricating on a real silicon solar cell, we simulated the solar cell performance using PC1D software. The reflectance spectra obtained from measurement were used in PC1D simulations to compare the effect on the short circuit current density (J_{SC}), open circuit voltage (V_{OC}) and efficiency (η) for a solar cell structure based on the standard PC1D template for a low cost silicon solar cell. The silicon material was set to p-type with resistivity of 1.008 Ω cm and a diffused emitter with error function distribution and 99.4 Ω/sq. emitter sheet resistances. The base contact had a resistance of 0.015 Ω and the cell had an internal shunt of 0.3 Siemens. The bulk life time was set to 7.03 µs with a front surface recombination velocity of 1800 cm/s and back surface recombination velocity of 25 cm/s [http://www.semiconductor.net/article/CA6572786.html]. The output characteristics and parameters obtained from PC1D for SLAR, DLAR and silicon nitride SWS are shown in Fig. 4. It is clear that J_{SC}, V_{OC} of silicon nitride SWS are higher than silicon nitride SLAR structure as seen from Fig. 4. A clear increase in efficiency of 0.8% can be seen for silicon solar cell with silicon nitride SWS over a cell with single layer silicon nitride ARCs and only 0.3% less in efficiency than the DLAR coated solar cell, which is believed to be due to lower reflectance of DLAR to silicon nitride SWS over the longer wavelength region (i.e. $\lambda > 600$ nm) that leads to lower short circuit current. From the above observations we can conclude that the efficiency of solar cell may not

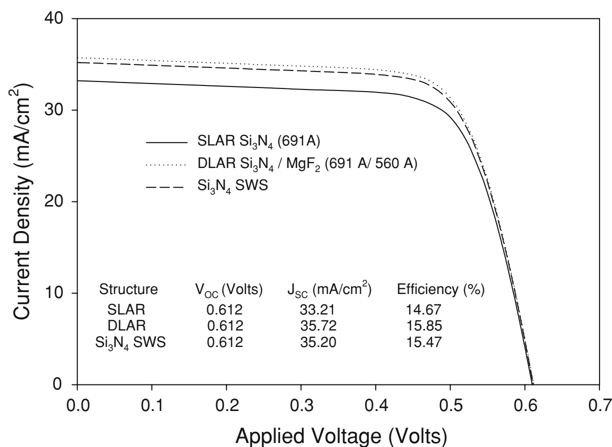

Fig. 4 PC1D Simulated solar characteristics for silicon nitride SWS, silicon nitride SLAR, and silicon nitride/MgF_2 DLAR

depend on the average reflectance, but, significantly on the reflectance of ARCs in longer wavelength region.

Conclusion

In summary, we have developed an easy and scalable non-lithographic approach for creating sub-wavelength structured antireflection coatings directly on silicon nitride antireflection coatings for the first time to improve the solar cell efficiency. PC1D simulated solar characteristics inferred that the efficiency increase of 0.8% for a silicon solar cell can be achieved using silicon nitride SWS over a cell with silicon nitride SLAR and a comparable performance with a cell with silicon nitride and MgF_2 DLAR.

Acknowledgments This work was supported in part by Taiwan National Science Council (NSC) under Contract NSC-97-2221-E-009-001-PAE, Motech Industries Inc. (MOTECH), Tainan, Taiwan, under 2008–2009 grants and by Laser application Department, Industrial Technology Research Institute, Hsinchu, Taiwan, under a 2008 grant.

References

1. L. Tsakalakos et al., J. Nanophotonics **1**, 1 (2007)
2. M.A. Green, *High Efficiency Silicon Solar Cells* (Trans Tech Publication, Aedermannsdorf, Switzerland, 1987)
3. S.M. Sze, *Semiconductor Devices, Physics and Technology* (Wiley, New York, 1985), p. 315
4. S. Strehlke, S. Bastide, J. Guillet, C. Levy-Clement, Mater. Sci. Eng. B **69**, 81 (2000). doi:10.1016/S0921-5107(99)00272-X
5. J. Zhao, A. Wang, P. Altermatt, M.A. Green, Appl. Phys. Lett. **66**, 3636 (1995). doi:10.1063/1.114124
6. S.E. Lee, S.W. Choi, J. Yi, Thin Solid Films **376**, 208 (2000). doi:10.1016/S0040-6090(00)01205-0
7. H. Sai, H. Fujii, K. Arafune, Y. Ohshita, M. Yamaguchi, Y. Kanamori, H. Yugami, Appl. Phys. Lett. **88**, 201116 (2006). doi:10.1063/1.2205173
8. P. Lalanne, G.M. Morris, Nanotechnology **8**, 53–56 (1997). doi:10.1088/0957-4484/8/2/002
9. Y.C. Chang, G.H. Mei, T.W. Chang, T.J. Wang, D.Z. Lin, C.K. Lee, Nanotechnology **18**, 285–303 (2007)
10. M.J. Minot, J. Opt. Soc. Am. **66**, 515 (1976). doi:10.1364/JOSA.66.000515
11. T. Glaser, A. Ihring, W. Morgenroth, N. Seifert, S. Schröter, V. Baier, Microsyst. Technol. **11**, 86–90 (2005)
12. D.H. Macdonald, A. Cuevas, M.J. Kerr, C. Samundsett, D. Ruby, S. Winderbaum, A. Leo, Sol. Energy **76**, 277–283 (2004). doi:10.1016/j.solener.2003.08.019
13. Y. Inomata, Sol. Energy Mater. Sol. Cells **48**, 237–242 (1997). doi:10.1016/S0927-0248(97)00106-2
14. H.F.W. Dekkers, Opto-Electron. Rev. **8**, 311–316 (2000)
15. M. Okuda, S. Matsutani, A. Asai, A. Yamano, K. Hatanaka, T. Hara and T. Nakagiri, SID Symp. Digest (2000) 185–188
16. B.G. Prevo, E.W. Hon, O.D. Velev, J. Mater. Chem. **17**, 791 (2007). doi:10.1039/b612734g
17. C. Aydin, A. Zaslavsky, G.J. Sonek, J. Goldstein, Appl. Phys. Lett. **80**, 2242 (2002). doi:10.1063/1.1466519
18. Y. Kanamori, E. Roy, Y. Chen, Microelectron. Eng. **78–79**, 287 (2005). doi:10.1016/j.mee.2004.12.039
19. Y. Kanamori, M. Sasaki, K. Hane, Opt. Lett. **24**, 1422 (1999). doi:10.1364/OL.24.001422
20. E.B. Grann, M.G. Moharam, D.A. Pommet, J. Opt. Soc. Am. A **12**, 333 (1995). doi:10.1364/JOSAA.12.000333
21. H.A. Macleod, *Thin-Film Optical Filters*, 3rd edn (Institute of Physics, Bistol, 2001)